H2Open Journal

IWA PUBLISHING

H2Open Journal Vol 5 No 2, 289 doi: 10.2166/h2oj.2022.003

Meandering rivers' morphological changes analysis and prediction – a case study of Barak river, Assam

Apurba Nath* and Susmita Ghosh

Civil Engineering Department, National Institute of Technology Silchar, Silchar, Assam, India
*Corresponding author. E-mail: apurba_rs@civil.nits.ac.in

ABSTRACT

Morphological studies are vital for water resources management, riverbank development, and flood mitigation. In this study, the sinuosity index and bank erosion were used to detect and quantify morphological changes using Landsat data (1990–2020) in the Barak river, India. The morphological changes were investigated in protected areas to analyze the effectiveness of existing protective structures on bank migration, which helps formulate better riverbank restoration plans. Using monthly discharge data from two stream gauge stations, the Seasonal Autoregressive Integrated Moving Average (SARIMA) models were developed. The extensive sediment transportation in the region necessitates studying both the river flow and morphological changes. The developed SARIMA model was used to predict river discharges up to 2025, being trained with data from 2006 to 2015. The validation of the model (2016–2018) shows that the mean absolute percentage error for discharge at two gauging stations is 29.78 and 23.52%, respectively. The analysis shows that the sinuosity index and bank erosion were inversely proportional. The SARIMA model showed that the future monthly discharge in the case study could be substantially higher than the observed series and affect river erosion simultaneously. This approach applies to many other meandering river management and identifies future morphological changes.

Key words: meandering river management, river morphology, river protection structure, SARIMA model, sinuosity index

HIGHLIGHTS

- Sinuosity index and riverbank erosion both are inversely proportional.
- The efficiency of protection structures must be determined for alluvial river management. Inadequate protection structure planning might lead to downstream hazards.
- The SARIMA model can accurately estimate future discharge by which segment-by-segment future morphological analyses are possible.

GRAPHICAL ABSTRACT

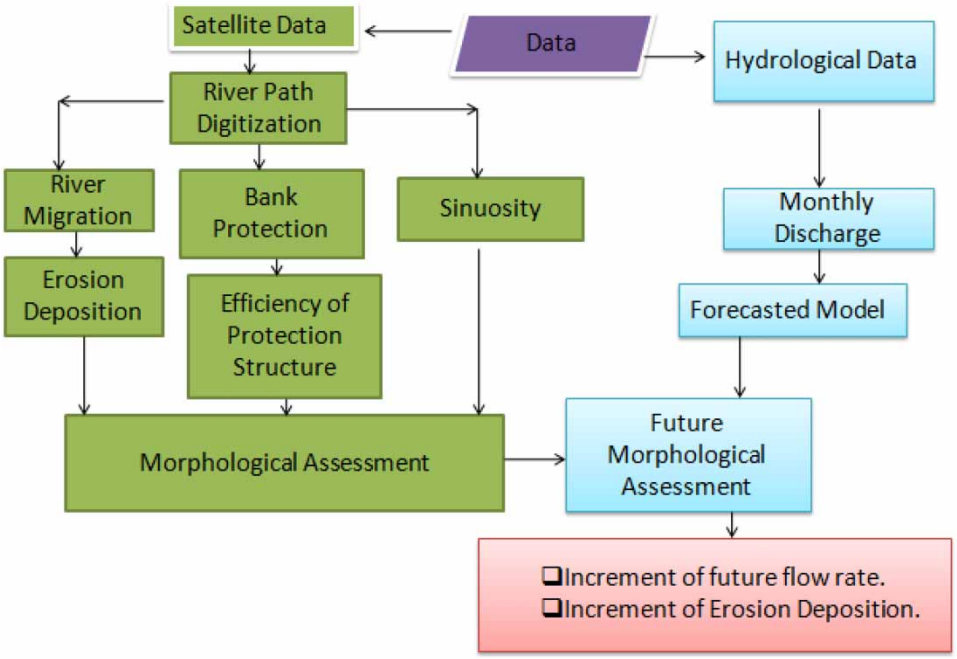

1. INTRODUCTION

Bank erosion is a natural phenomenon for meandering rivers in alluvial stretches. The meandering rivers undergo morphological changes due to bank erosion and sedimentation from banks and beds. Hence, it is required to study the rivers' morphological changes. The sinuosity index and bank erosion are used to detect and quantify the morphological changes in rivers (Schumm 1963; Ozturk & Sesli 2015). The river drainage line's sinuosity index measures the river's impact on terrain (Panda & Bora 1992). Bank erosion, accretion, and channel alteration are closely linked to climate change, discharge amount, type of bed material, and fluctuations in the hydrologic cycle.

Riverbank erosion is an endemic disaster that has a long-term impact on various natural disasters (Das *et al.* 2014). Stream-bank erosion and its consequences on channel evolution are important geomorphic research issues that have applications in various scientific and engineering sectors. It has several socio-economic adverse effects, like Serbian farmers losing their productive lands on the left bank of the Danube river because of flooding (Dragicevic *et al.* 2012). Bank erosion in Padma and Jamuna rivers in Bangladesh between 1970 and 2000 displaced more than two lakhs people from their residential area (Islam & Rashid 2011). The morphological change in the Ganga River near Allahabad, India was studied (Pati *et al.* 2008). According to the National Disaster Management Authority, India (2014), Bihar and Assam were two of India's most heavily flooded and erosion-affected states. Collaborated study by Space Application Centre (SAC), Ahmedabad, India, and the Brahmaputra Board, India (SAC and Brahmaputra Board 1996) determine the impacts of river erosion on Majuli Island, to identify and delineate the island portions that had changed along the bank line due to the river's dynamic behavior. Remote sensing data were analyzed using the GIS tool to quantify bank erosion in the Brahmaputra River at Agyathuri, Assam, India (Bhakal *et al.* 2005) for 30 years, from 1973 to 2003. Landsat-MSS, TM, and ETM images were used to analyze the changes in the Brahmaputra river flow between 1970 and 2002 (Das & Saraf 2007).

The Barak river, which flows parallel to the Brahmaputra in the southeast part of the Himalayan range in northeastern India, is the country's second-largest river, covering around 1.38% of the country's total geographical area. The Barak river's discharge and sediment carrying capacity have increased in recent years (Annayat & Sil 2020a). The Barak River's channel behavior was analyzed using satellite imagery and some field data to find river segments that remained steady between 1910 and 1988 (Bardhan 1993). Barak river's quantitative analysis revealed an upward trend in erosion and deposition was observed between 1918 and 2003 (Laskar & Phukon 2012). The study was performed to evaluate the degree of flow controls required in upstream catchments to

provide safe flow at downstream damage locations in the Barak river (Choudhury *et al.* 2014) used to detect the changes in the planform features of the river Barak Moreover, major bank shifting in the Barak river was analyzed, the study predicts that it will have disastrous effects on the economy and livelihood of the people soon (Annayat & Sil 2020a). The study was performed to describe and assess the empirical technique and time sequence extrapolation method for channel width prediction over Barak (Annayat & Sil 2020b).

During the post-independence period, Assam experienced catastrophic floods in 1954, 1962, 1972, 1977, 1984, 1998, 2002, 2004, and 2012 (Kipgen & Pegu 2018). Due to flooding, huge bank erosion occurred in the Brahmaputra and Barak valleys, Assam. Assam lost 868 km^2 of land due to bank erosion between 1912 and 1996, an average loss of 10.3 km^2 each year (Sharma *et al.* 2010). Spatial analytic technologies such as geographic information systems (GIS) and remote sensing (RS) can be used efficiently for the accurate identification of flood extent and depths within flood plains, which are crucial for proper flood management (Sahoo & Pekkat 2018). Many remote sensing studies were done on major rivers worldwide (Rinaldi 2003; Yang *et al.* 1999; Kummu *et al.* 2008; Surian *et al.* 2009; Betancourt-Suárez *et al.* 2021). Therefore, it is revealed from the previous literature that one of the key reasons for bank erosion is the occurrence of high floods in the alluvial channel (Lane *et al.* 1995). Flood risk increases when the sinuosity of the stream decreases, and river banks fail when downward driving forces exceed resisting forces (Mohammed-Ali *et al.* 2020).

The study of flood forecasting and warning system was increased due to the increasing impact of high flooding since the late 1980s. For the safe and cost-effective design of river engineering works, a precise estimate of a flood of a specific recurrence period at a site is typically required (Prabhata *et al.* 1995). The hydrological, environmental, and societal effect was studied to identify the effect of flood risk (Kumar & Bhattacharjya 2020). The need for more accurate time series forecast models has prompted researchers to develop improved methods for modeling time series and tackling non-linearity issues (WMO 2011). The frequency and amount of peak flow affect the planning and design of water resource projects and flood-plain management (Thalla *et al.* 2010).

Thus, a watershed's average discharge represents the potential water resources used, and the utilization strategy must be structured accordingly. Because river discharge has a predictable pattern over time, a time series model can express the river discharge pattern mathematically (Mosavi *et al.* 2018). Autoregressive Integrated Moving Average (ARIMA) model is one of these widely used linear time series models (Box & Jenkins 1976). The stochastic ARIMA models were applied for large European rivers to predict stream discharge. Results show that this model was suitable for hydrological simulations for European rivers (Stojković *et al.* 2015). The ARIMA model's applicability to monthly flow series was investigated (Yurekli *et al.* 2005). The model was applied to forecast what would happen without knowing other influencing factors. When communities and organizations are prepared to reduce damage from severe, widespread, and unexpected floods, these effective flood warning and flood forecasting programs are beneficial. The seasonal variations in the ARIMA time series are strong and uneven; as a result, this series is highly variable (Moeeni & Bonakdari 2010). This study provides the model to anticipate this series type and predict the upcoming monthly discharge. The Seasonal Autoregressive Integrated Moving Average (SARIMA) is a time series model used for predicting future time series based on the previous trend of data. The SARIMA model was developed by integrating the AR and MA models, as well the AR and MA models. The highly variable time series is represented by the Seasonal SARIMA model (Sharma *et al.* 2020). When the time series data show seasonal characteristics, SARIMA models are used, which combine seasonal differencing with an ARIMA model. The SARIMA hybrid model is used instead of the ARIMA model due to the seasonality of the time series (Zhang 2003).

From previous literature, it has been concluded the Barak flood plain in the Cachar region has suffered regularly due to catastrophic floods. So a flood model is required to analyze the flood risk for this region. The SARIMA model can be applied to the Barak River in the Cacharregion for analyzing and predicting monthly discharge patterns to analyze the flood risk. For river stability, discharge-morphology behavior and future morphological consequences are essential, especially for the highly migrating river like the Barak. No studies have identified the future discharge time series with a high seasonal variance model and the output of the prediction model was applied to assess the future morphological changes. It is critical to establish and implement an emergency action plan with suitable structural protection planning in advance to prevent future river morphological changes.

Standard bank protection methods are used to reduce river migration. These strategies aim to provide safe and efficient water and sediment conveyance (Klassen & Verneer 1988). Therefore, the efficiency of protection structure within alluvial reach is also important for assessing the river discharge and forecasting the river morphology.

A geomorphic evaluation was used to give baseline data used to characterize river morphological changes. River morphological changes concern the position of river control points and reach dynamics and divide the channel into discrete sub-reaches with similar morphology.

Floods are a recurring issue in the Cachar region, Assam, India. Every year floods devastate large areas, destroying property and crops and disrupting communications due to erosion (Das 2012; Choudhury *et al.* 2014). The amount of bank erosion fluctuates from year to year, depending on the intensity of the state's floods. Assam is a state in northern India that is less developed than the rest of the country. The region has 652.3 billion m^3 of surface water (a large portion of which comes from the Brahmaputra-Barak River System), accounting for 34% of the country's total water resources (Das 2013). Bank erosion frequently occurs in the alluvial river plains, causing it to change course. Moreover, a significant bank shifting was observed on the Barak river (Das 2012). Hence, a huge amount of river migration was observed within this part of the river.

1.1. Present study

In the present study, an analysis of morphological changes in Barak river was performed to quantify the changes in the spatial and temporal variation of sinuosity index and their effect on morphological characteristics. The model was further applied to predict future morphological changes in rivers.

The study's first goal is to analyze the morphological changes of the region and understand the morphological changing behavior of river Barak by computing segment-wise sinuosity index and bank erosion using remote sensing data. The erosion-prone zones within the river stretch were also identified. Due to river stability concerns, one of the primary concerns of the morphological study was to assess the effectiveness of recently protected regions within the region. The second goal is to develop the SARIMA model that uses seasonal differencing to forecast monthly river discharge. The SARIMA model forecasted output was also used to perform morphological changes forecasting. This study aids the water resources managers and decision-makers make an efficient plan for meandering river management.

1.2. Study area

River Barak flows from the Naga Hills' Barail Range at an elevation of around 2,995 m into Assam at 24° N latitude and 93° E longitude. The river Barak was divided by Surma and Kushiyara to make its way to Bangladesh. The river Barak, which flows through India's tropical region, contains several abandoned meandering loops and decadal shifting. The Barak river has around 900 km long; out of this 532 km are in India, and the rest are in Bangladesh. Out of 532 km of India, 129 km followed the Barak valley in Assam. The Barak valley has a width of around 25–30 km and is located in the southwest monsoon zone (Choudhury *et al.* 2014). The main tributaries of the river Barak are Katakhal, Jiri, Chiri, Modhura, Longan, Sonai, Rukni, and Singla. Throughout the Barak valley, the Barak river's channel position has varied significantly, with a considerable northward trend to the west of Silchar (Das 2012). Multiple erosion events resulted in river migration for most of the study period since the river course followed a sharp meandering pattern. As alluvial rivers erode and deposit silt along their banks, meanders flow through flood plains, resulting in course changes. Because of the significant sinuosity and erosion in the study area, cut-off formation is always possible. Therefore, a long time planning for mitigating flood and erosion damage is required. Silchar is one of the busiest towns in northeast India, located in the Barak valley of Assam. It is the major commercial center for Tripura, Manipur, Mizoram, and Southern Assam. So, planning for mitigating flood and erosion damage is required particularly for this highly important town and its surrounding areas. So, the Barak river stretch near the Silchar town between Jirimukh and Uttar Badarpur was considered the study area (Figure 1). This river stretch has about 25 steep bends between the Jirimukh to Uttar Badarpur. A menders loop surrounds half of the area limits in Silchar town, and the protective construction protects only a few out of these bends. As a result, this section of the valley experiences significant migration.

2. MATERIAL AND TECHNIQUES

2.1. Data collection

In this study, two types of data were used: satellite data and hydrological data. The multispectral remotely sensed data and multi-temporal Landsat data were obtained from the United States Geological Survey (USGS). Every 10 years, Landsat images were collected from 1990 to 2020 (Table 1). Monthly discharge data from 2006 to 2018 were collected for two-stream gauge stations on Barak River named Annapurnaghat and Badarpurghat.

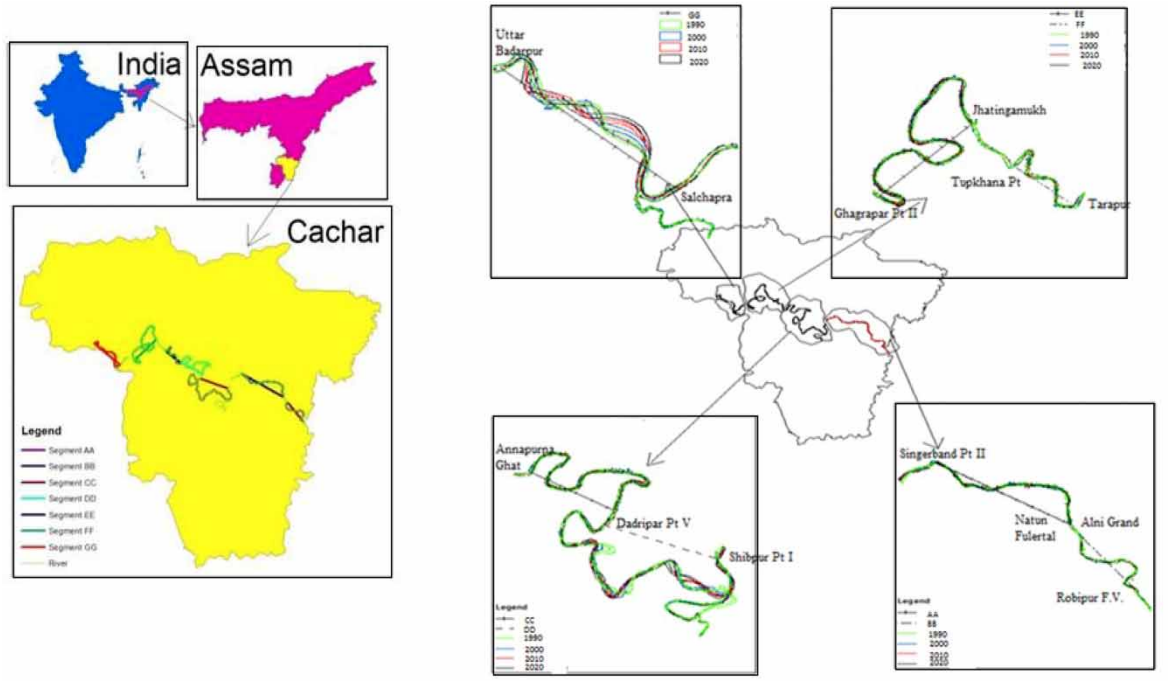

Figure 1 | Study area map.

Table 1 | Satellite data was used in the study

Spacecraft ID	Landsat 5	Landsat 7	Landsat 7	Landsat 8
Year	1990	2000	2010	2020
Sensor ID	TM	ETM +	ETM +	ETM +
WRS path	146	146	146	146
WRS row	43	43	43	43
Resolution (m)	30 × 30	30 × 30	30 × 30	30 × 30

Information about the research area's protection zone was taken from the Cachar division, Department of Water Resource, Government of Assam, and a local field visit.

2.2. Technique

Two types of analysis were done in this study. The first was to analyze the morphological changes concerning changes in the sinuosity index correlated to bank erosion and the second was to forecast morphological changes by predicting river discharges using the SARIMA model. The methodology used for the study was shown in the flow chart (Figure 2).

2.2.1. Morphological assessment

The sinuosity index is one of the most important factors to consider in identifying morphological changes in rivers throughout time. Sinuosity addresses the river's meandering nature. It is the ratio of the actual length of the river to the straight length (Equation (1)) (Schumm 1963).

$$SI = \frac{CL}{EL} \tag{1}$$

where CL is the curvature length and EL is the Euclidean length.

The sinuosity index was calculated by layer stacking different bands in ArcMap. Each decade Landsat images were then further pre-processed and digitalized. After digitizing river courses, sinuosity was calculated by dividing

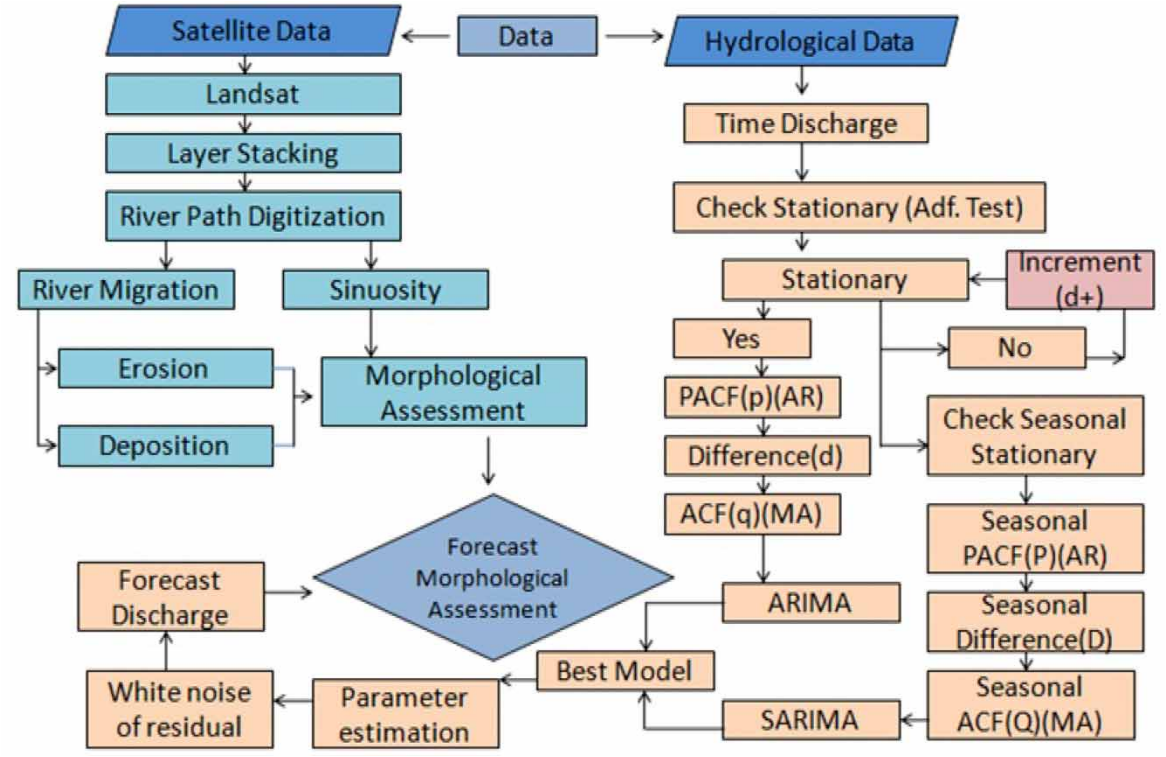

Figure 2 | Flowchart of analysis.

curvature length by the expected Euclidean length. The flowchart (Figure 2) shows the steps involved in calculating the sinuosity index.

Riverbank erosion over time is monitored by the indirect method using satellite data. New river configurations, river channel changes/river migration, and riverbank erosion/deposition were tracked using multi-temporal high-resolution satellite data (Figure 2). For the years 1990–2020, Landsat images were used to analyze river migration and the river's sinuosity index. The effectiveness of the protection structure, as well as its effect, were then studied in understanding the protected area's behavior.

In this case, time series analysis was used to identify the data's historical pattern and develop an ideal forecasting model. The forecasting model's output was used to estimate the study area's future morphological changes.

2.2.2. Forecast morphological changes

River discharge forecasting is essential for the morphological assessments of meandering rivers. Therefore, discharge data were used for forecasting stream flow and future morphological changes. ARIMA and SARIMA models were widely used to predict time series analysis. Data should be split into trend, periodicity, autoregressive, and random components in stochastic modeling techniques. The model ARIMA (p, d, q) was summarized as the combination of the three – autoregressive order p, the moving average process of order q, and d representing an order of differencing (Galavi *et al.* 2013). The SARIMA model applies the ARIMA models to a modified time series. SARIMA model covers autoregressive and random component modeling after removing trend and periodical components seasonally. The non-seasonal and seasonal parts of the model are (p, d, q) and (P, D, Q)s, respectively. A SARIMA model follows Equation (2) (Chatfield 2000).

$$\alpha(B)\emptyset(B^s)(1-B)^d(1-B^s)^D X_t = \theta(B)\vartheta(B^s)Z_t \tag{2}$$

where $\emptyset(B^s)$ and $\vartheta(B^s)$) denoted polynomial of B^s with P and Q order; $\alpha(B)$ and $\theta(B)$ the denoted polynomial of B with p and q order.

Four steps are followed for model development as follows – identification, estimation, verification, and application or forecast to find the optimal forecast model for each station. Initially, the data stationarity was verified, and the general form or model order was estimated. Then the model parameters were calculated using maximum

likelihood, and the model's appropriateness was tested using the Ljung–Box statistical test. The best model was chosen from those that fit the data well. The Akaike Information Criterion (AIC) was used to select the optimum model (Martínez-Acosta *et al.* 2020). Each model's AIC was computed, and the lowest AIC was chosen for further future morphological changes. Finally, the optimal model was selected for the forecast. The results were compared with the observed value, and uncertainty performance was assessed by the two statistical indices – coefficient of determination (R^2) and mean absolute percentage error (MAEP). The model was further applied to forecast the future morphological changes over the region.

3. RESULTS

3.1. Morphological assessment

3.1.1. Sinuosity index analysis

A stretch across the river valley within the study region was chosen with a length of roughly 134 km to understand better the river Barak's migration characteristics. The river was separated into seven segments for sinuosity computation (AA, BB, CC, DD, EE, FF, GG), which begin upstream at Robipur F.V (near the Manipur border) and end in Uttar Badarrpur (Uttar Badarpur). The sinuosity map shows 1990–2019 (Figure 1). The sinuosity index of each segment was calculated using ArcMap software over 10 years for each portion. A few critical locations (Table 2) considering vulnerability along river segments were included in the study area.

Segment AA, from Robipur F.V. to Alni Grand, and Segment BB, from Natunfulertl to Singerband Pt II, were the most stable segments (Figure 3(a)). River migration was less, and the sinuosity index graph was more linear.

Segment CC, which extends from Shibpur Pt I to Dadripar Pt V, and segment DD, which was runs from Dadripar Pt V to Annapurnaghat, were the next two segments. Because they cover most Silchar township regions, these portions require more attention than others. According to the sinuosity study, the average sinuosity for both sections was 3.88 and 2.83, respectively. They indicate a highly meandering stretch where segment CC was most vulnerable within the study area. The next segment EE was considered for the Sinuosity study. It was run from upstream Tarapur to Tupkhana Pt I, followed by the segment FF, which was run from Jhatingamukh to Ghagrapar Pt II. Segment EE has a sinuosity of 1.66, whereas segment FF has a sinuosity of 3.13. The segment sinuosity line straightness almost follows the same path through time, indicating no previous migration events. However, a modest drop in sinuosity has been discovered in section FF over the last decade, indicating an increase in riverbank erosion. Segment EE and segment FF followed exceedingly meandering curves. As a result, according to the river stability concept, even little variations in sinuosity can produce serious erosion difficulties. Segment GG, which runs from upstream Salchapra to downstream Uttar Badarpur, was vulnerable. The Average Sinuosity of the segment was 1.44, which was lower than that of several upstream segments. Despite this, after digitizing the river path, it was discovered that this stretch of the river path had been influenced by significant river migration activities over the last decades, with massive migration and deposition processes influenced the land throughout the study.

Table 2 | Important locations are included in the study area

Segments	Area covered	Important banks
AA	Robipur F.V. to Alni Grand	Rabipur, Lowarjiri Pt V, Alni Grand.
BB	NatunFulertal to Singerband Pt II	Fulertal, Kaptanpur Pt V, Singerband.
CC	Shibpur Pt I to Dadripar Pt V	Shibpur Pt I, Singerbond Pt III, Kaptanpur Pt I, Sonaimukh, Jhanjarbali, Bagpur, Govindapur, Sonabarighat, Saidpur, Dhamalia, Dadripar Pt V
DD	Dadripar Pt V to AnapurnaGhat	Berenga Pt V, Kasipur Grant, Berenga Pt III, Kanakpur, Dadripar, Madhurband Ambikapur Pt X Anapurna Ghat.
EE	Tarapur to Tupkhana Pt I	Tarapur, Dudhpatil, Nathpara, Masughat, Tupkhana Pt I.
FF	Jhatingamukh to Ghagrapar Pt II	Jhatingamukh, Bhairabnagar, Raipur, Nischintapur, Buribali, Ganigram, Ghagrapar Pt II.
GG	Salchapra to Uttar Badarpur	Salchapra, Sripur Pt II, NizFulbari, Pachgram, Uttarbadarpur.

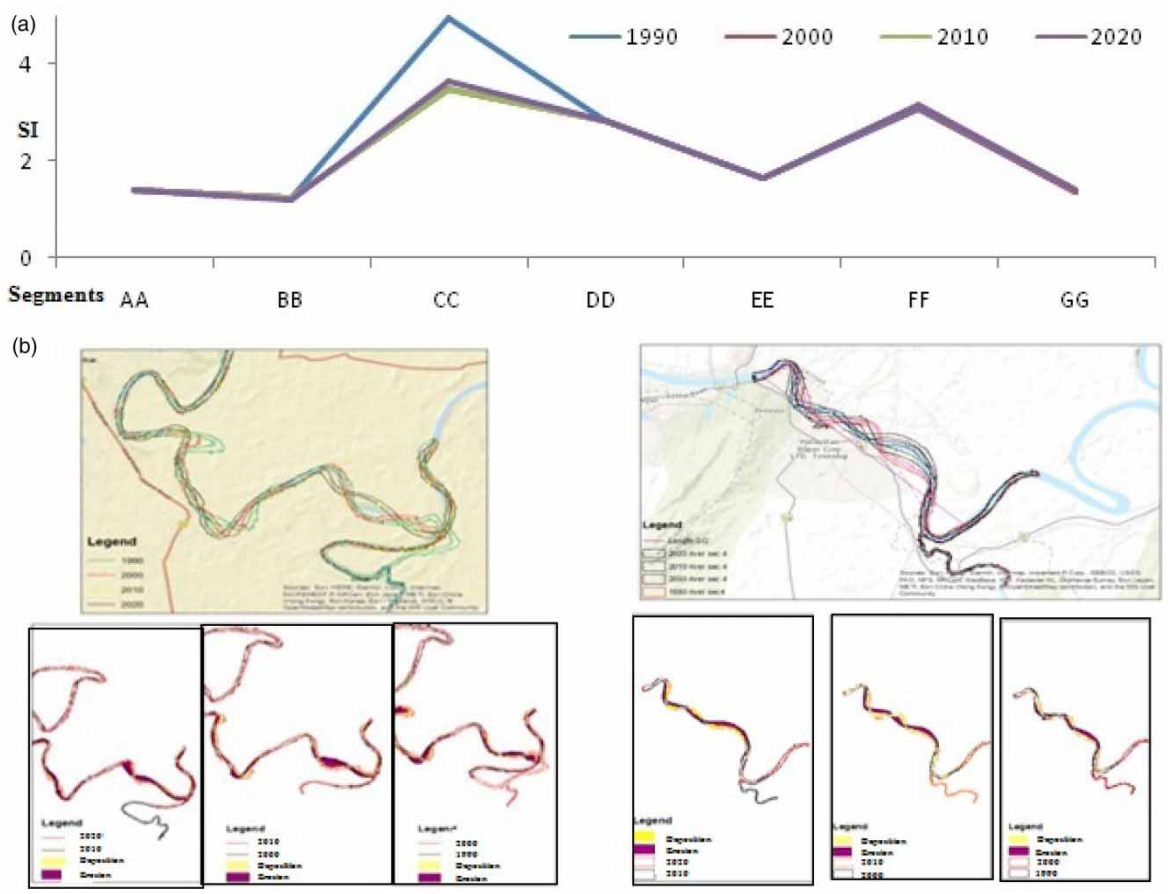

Figure 3 | (a) Sinuosity Index Segment-wise. (b) Most vulnerable segment within the study area (Segment CC, GG).

Compared to other segments, segment CC has the highest and most crucial sinuosity index, although there was a massive river migration throughout the study period. Between 2010 and 2020, this value is extremely high. Segment AA has been the most stable part of the study.

3.1.2. Morphological changes due to segment-wise sinuosity changes and corresponding erosion deposition activity

Figure 3(b) shows the activities of erosion deposition for all segments. Segments CC and GG, where past migration has altered the land throughout the study period, were the most vulnerable zones in the study area. The activities of erosion deposition were related to sinuosity for all segments. It was necessary to understand the relation between sinuosity and river migration. The erosion deposition investigation was carried out throughout the segments better to understand morphological changes and their relationship with sinuosity (Figure 4).

As per sinuosity analysis, both sections were relatively stable for segment AA and segment BB compared to other segments within the study area. Due to increased erosion activities between 1990 and 2000 (Singerband Pt II), a protective structure was constructed here under section BB.

Sinuosity analysis showed significant fluctuation over the decade in segments CC (Figure 3(a)). As a result, that zone's variability was rather significant, particularly for segment CC, as shown in Figure 4(c). Several migration activities had been noticed in the segment CC over the study period. The rate of migration has also fluctuated over the years. Erosion deposition activities were tracked over time to identify morphological changes concerning sinuosity in rivers over the decade was analyzed. Oxbow generation was one of the key morphological changes over the segment. The river path was cut off from the main Barak near Sonaimukh (Kaptanpur) during 1990–2000. The introduction of cutoff has resulted in a length reduction. The creation of the oxbow resulted in the loss of a 10-km stretch of river from the main Barak river. Within segment CC, the most affected areas were identified as Jhanjharbali, Govindapur, Sonabarighat Pt II, and Sonabarighat Pt I, where historical river migrations using satellite data were recorded over the study period. A field visit was done in those erosion-prone areas to

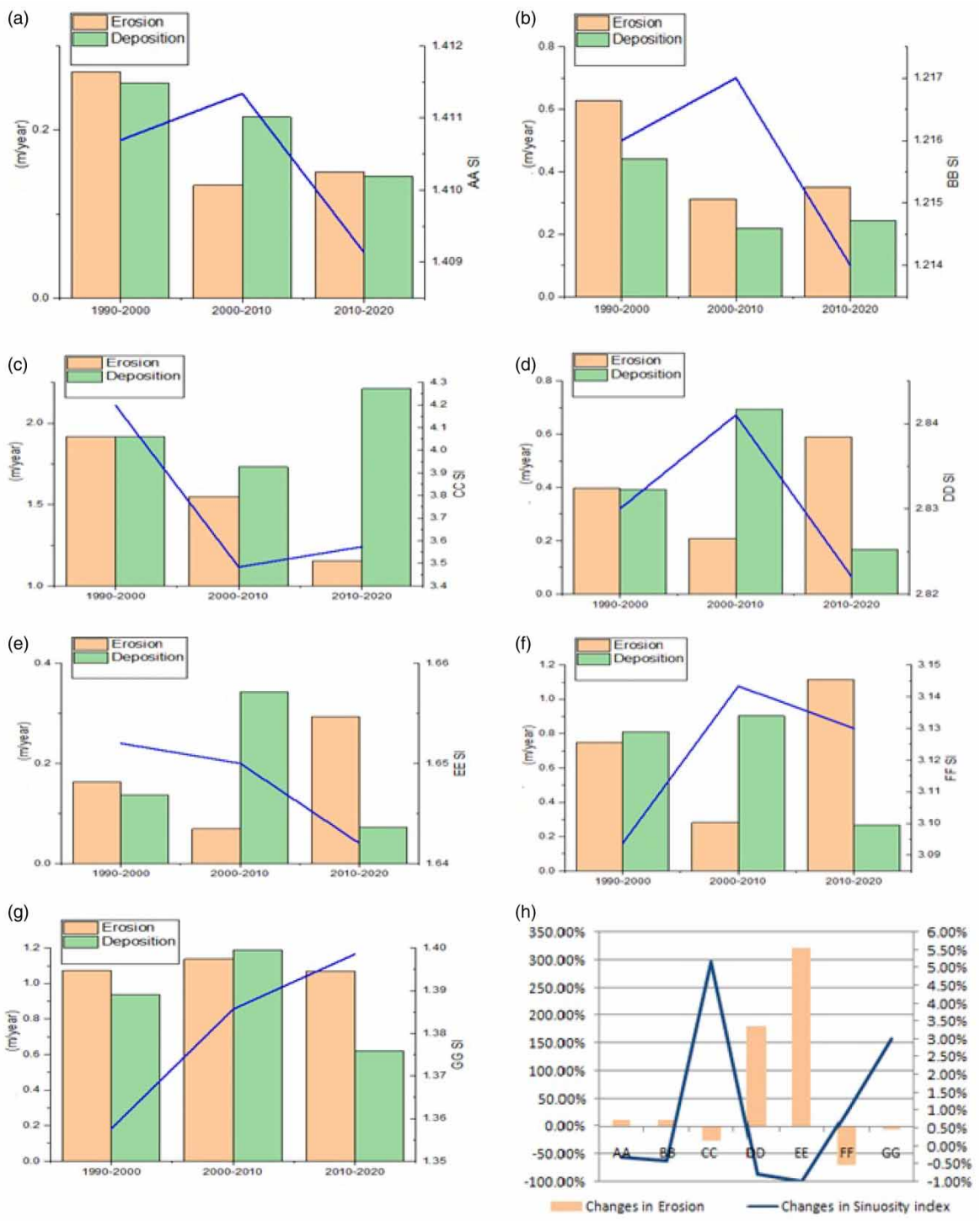

Figure 4 | (a) Erosion deposition relation with sinuosity segment AA. (b) Erosion deposition relation with sinuosity segment BB. (c) Erosion deposition relation with sinuosity segment CC. (d) Erosion deposition relation with sinuosity segment DD. (e) Erosion deposition relation with sinuosity segment EE. (f) Erosion deposition relation with sinuosity segment FF. (g) Erosion deposition relation with sinuosity segment GG. (h) Relationship between changes in sinuosity and changes in erosion over the decade (2010–2020).

verify the fact. More than 37 m of yearly shifting at Jhanjharbali and more than 50 m of yearly shifting near Govindapur had been observed, making the zone more vulnerable. Due to huge migration activities, a roadway near Govindapurwas completely failed in between the last decade observed during the field visit.

The portion between Dadripar and Tarapur is referred to as Segment DD, and it was mostly followed a very little variation of sinuosity (Figure 4(d)). Even though some river sections were protected by riprap, erosion had substantially influenced the river during the last decade. As a result, sinuosity has decreased over the last decade. Most of the protected zones were established before 1990; and however, in light of current river conditions, they were ineffective. Within the zone, the protected banks were Madhurband, Annapurnaghat, and Ambikapur Pt X. It has been analyzed that erosion activities had grown during the last decade. Hence, the government has lately adopted Geo-bag protection steps to protect those banks. Baghadhar, in particular, was one of the most damaged regions in this section, with prior erosion activities that could contribute to future oxbow formation.

For segment EE, because of protective features on multiple major bends within this sector of the study area, there was less river movement in this region of the study area than in the upstream portion of the river, resulting in less variance in Sinuosity analyses (Figure 4(e)). The terrain becomes more prone to river erosion when sinuosity decreases. However, because the quantity of erosion was minor, little protection might help maintain river stability.

For segment FF, the major sharp bends of Dudhpatilghat, Tarapur Pt V, and Masughat were protected by protection measures. There were no such historical movements observed per river morphological analysis, but still, a sharp increment of erosion was observed during the last decade (Figure 4(f)).

In segment GG, a significant impact on river migration in various segment parts was observed from digitized river paths from 1990 to 2020 (Figure 4(g)). Sinuosity has increased during the last decade, implying a decrease in erosion activity. Nonetheless, there was a lot of migration in this area. Sripur I, Sripur II, NizFulbari, Kalinagar, and Pachgram were the erosion-affected regions within the segments as per historical data.

The sinuosity analysis (Figure 4(a)–4(g)) shows that even minor sinuosity variations had a significant impact on river movement (Figure 4(h)). However, the increase in sinuosity was due to riverbank deposition. A slight decrease in sinuosity across any segment has a significant eroding effect on river morphology. That means sinuosity and erosion were a vice versa relationship with each other.

3.1.3. Protective structure and its effect on river migration

According to river migration studies done throughout the region (Figure 4(a)), the land under segment AA has been well protected from river migration. One of the most important variables influencing erosion is hydrological parameters. Therefore, an investigation yields a comprehensive understanding of erosion causes. For discharge, data from the Lakhipur river gauge station, located within section BB, were collected from 1975 to 2010. According to a hydrological assessment, the land was damaged by a high flow stage between 1989 and 1990 (18.7 m). However, the average river stage over the stretch was 17.38 m, significantly higher than normal. Therefore, the erosion statistics decreased after a protection structure was erected over segment BB between 1990 and 2000. It was also related to the efficiency of the protective measures over the segment. However, in 2006, the land area again faced a high flow level (21.6 m), the highest flow level that the land had experienced during the study period. But due to the protective structure, the erosion effect was not significant compared to earlier high floods. The land protects the erosion quite satisfactorily as morphological assessment of this portion analyzed.

However, there has been a decrease in erosion over time, particularly since the last decade for segment CC. According to information gathered throughout the region, Sonabarighat Pt II was one of the most affected areas where protection measures were implemented after 2010. As a result of the significant reduction in erosion activities, the protection structure has become more effective in river migration management. Therefore, an erosion deposition study also determines the effeteness of the protective structure over the zone. The downstream effect like segment CC due to protection structure similar situation was also observed in the segment GG. The erosion reduction was also reported after constructing protection measures near Sripur Pt II (Figure 5(a)).

Due to the existence of NH53 near the river bank, this part of Bends now has greater importance for Pachgram than other sites. The only road that connects Silchar to the rest of the country is situated within the segment GG. Until 2015, residents of Silchar and the neighboring areas suffered each year when the roads at Pachgram were shut off due to significant erosion during or after floods. Riprap mat protection, Porcupine, and group pile were recently employed to protect the area from bank erosion (after 2015). As a result, a significant reduction in erosion activity over some highly vulnerable historical bends (Figure 5(a)).

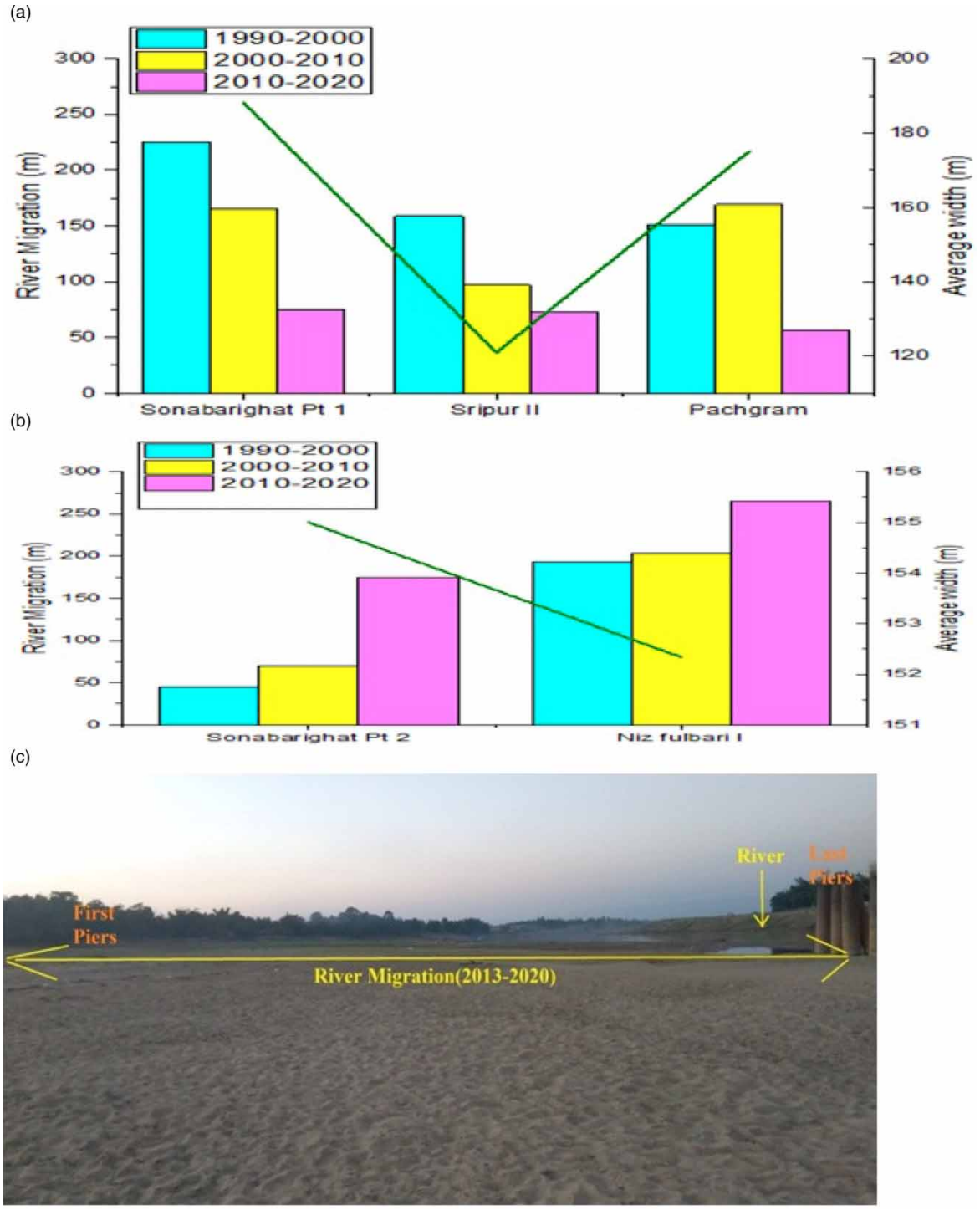

Figure 5 | (a) Workability of protection structure, (b) downstream effect of Protection Structure (c) field visit in the downstream effect of Protection Structure.

After installation of the protection structure, it makes the portion more stable, and erosion structures are also working properly during high stage flow period. And therefore, an increment of sinuosity over the period was also observed.

The river migration was controlled very efficiently all across the place by the protection construction near Sonabarighat Pt I (Figure 5(a)). It was estimated that about two-thirds of erosion impacts were mitigated by constructing riprap protection over the bank. However, some of the protection structure's effects were shifted to the river's downstream section around Sonabarighat Pt II. Although, it was observed from the present analysis that the vulnerable zone was protected by installing a river protection measure. But, a significant migration effect has been noticed near the downstream of the protective structure (Figure 5(b)). This land (Sonabarighat Pt II) has

been subjected to significant migration due to the influence of the upstream protective structure near Sonabarighat Pt I since the last decade. Piers were built here between 2012 and 2013 (Figure 5(b)), which were used to connect the two ends of the river in preparation for constructing a bridge. As per collective information, due to some issues, the construction activities were suspended in 2013. Over a decade, the river has moved an enormous amount of land, reaching the last piers of the bridge. Here, over 150-m migration was observed within the last decade. Nonetheless, massive migrations impacted this region (Figure 5(c)).

The downstream effect like segment GG due to protection structure was also observed in the section. Hereafter, due to the installation of a protection measure near Sripur Pt II, reduction of erosion was also notified (Figure 5(b)). But more instability toward downstream was observed. An increase in erosion activities downstream was seen due to the protection measures (NizFulbari).

3.2. Forecast morphological assessment

3.2.1. Discharge forecasting model

Monthly discharge data was acquired from Annapurnaghat and Badarpurghat, two river gauge stations located within the study area. First, a Box–Cox data transformation was used to ensure that the series was normal. Then, for validation, the Augmented Dickey–Fuller test (ADF) was utilized, a unit root test that permits accepting or rejecting the null hypothesis of stationarity in a time series.

Peaks may be seen once a year in the Annapurnaghat and Badarpurghat station transformed series graph (Figure 6), indicating that the series has seasonal characteristics. However, decomposing the time series allows determining the series components (trend, seasonality, random components) and examining their structure.

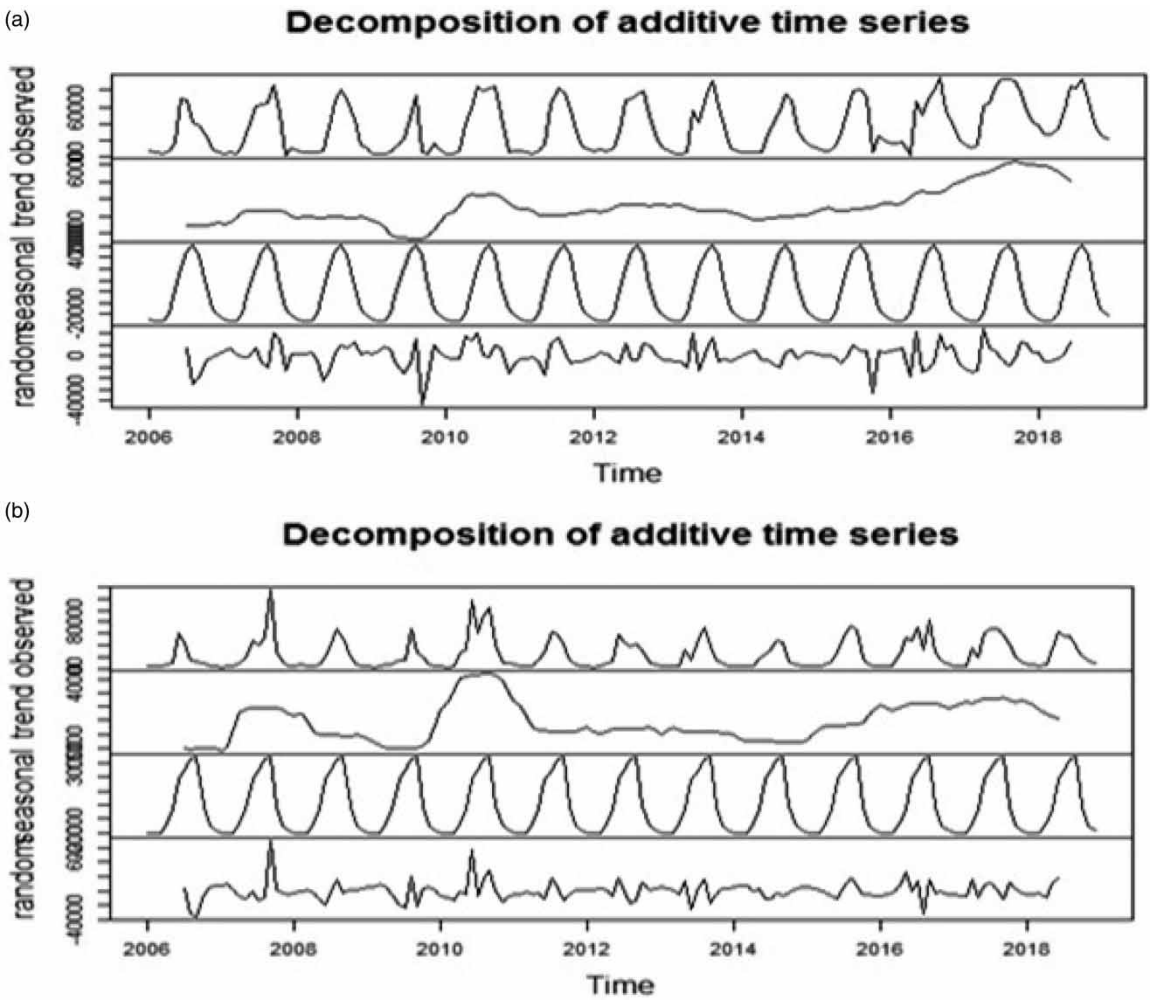

Figure 6 | Decomposition of calibration vector of the transform discharge time series for Annapurna and Badarpurghat station trans using Box–Cox (Time series graph with trend, seasonality, and random components).

Model Identification: In light of this, we can deduce that $s = 12$, i.e., the number of periods every year is 12 (one period per month). The series correlograms were calculated from the ACF and the PACF to check the latter.

The correlograms also imply that the SARIMA model best fits the gauge station and the weather station. Table 3 shows the correlogram plot (ACF, PACF) for the monthly discharge data set. The appropriate values of P, p for the autoregressive model and Q, q for the moving average model were determined using these plots.

For both the station and the p, d, q, P, D, Q values, various models were developed.

The Ljung–Box test and correlograms (Table 4) were then used to assess the residuals for the best model.

This statistical test was used to see if any time series autocorrelation group differed from zero. Using Ljung–Box statistics, the residual coefficients were found to be non-significant. Both Ljung–Box and Box–Pierce tests had probability values above 0.05, indicating non-significant. A non-significant value indicates a good fit.

The results of the residual test for the best model were very much satisfied for Annapurnaghat station as model order $(1,0,1)(2,1,1)_{12}$ and for Badarpurghat station the model $(2,0,0)(1,1,1)_{12}$ residual much better than $(1,0,0)(1,1,1)_{12}$ (Figure 7). Therefore model $(2,0,0)(1,1,1)_{12}$ was used for forecasting purpose. So, the best models were chosen to anticipate the discharge for 2019–2025. The forecasted values had confidence limits. The selected model's expected value was compared to the observed value to validate the model shown in Figure 8(b,d).

To demonstrate the performance of the chosen model, the figure shows the expected and actual series in a single plot, and their uncertainty was performed in Table 5. The model worked successfully for the Badarpurghat stream river station, in contrast to the Annapurnaghat stream gauge station. This was because the discharge at Annapurnaghat was significantly higher in the last few years of data collection than it was at the start of the series. As indicated in the validation of the model, the forecasted model was still computed more or less precisely.

Table 3 | Correlograms data of time series

		Annapurnaghat		Badarpurghat	
Order	**Lag**	**PACF**	**ACF**	**PACF**	**ACF**
0	0	0	1	0	1
1	0.0833	0.765	0.765	0.589	0.589
2	0.1667	−0.377	0.429	−0.065	0.304
3	0.25	−0.256	0.072	−0.193	0.027
4	0.3333	−0.231	−0.249	−0.252	−0.238
5	0.4167	−0.14	−0.469	−0.202	−0.411
6	0.5	−0.012	−0.531	−0.134	−0.463
7	0.5833	−0.092	−0.482	−0.105	−0.418
8	0.6667	0.183	−0.274	−0.053	−0.283
9	0.75	0.151	0.017	0.016	−0.082
10	0.8333	0.33	0.358	0.222	0.218
11	0.9167	0.211	0.622	0.144	0.417
12	1	0.103	0.721	0.11	0.502
13	1.0833	−0.012	0.619	−0.046	0.406
14	1.1667	−0.074	0.366	−0.133	0.181
15	1.25	−0.095	0.029	−0.107	−0.064
16	1.33	−0.062	−0.277	−0.159	−0.313
17	1.416	−0.029	−0.489	−0.024	−0.425
18	1.5	0.023	−0.554	−0.019	−0.447
19	1.5833	0.01	−0.478	−0.037	−0.394
20	1.666	−0.001	−0.278	−0.068	−0.261
21	1.75	−0.004	−0.001	0.007	−0.033

Table 4 | Selection of the best model

Annapurnaghat			Badarpurghat		
Model Identification	**AIC**	**BIC**	**Model Identification**	**AIC**	**BIC**
$(0,0,1)(1,1,1)^{12}$	3,184.19	3,196.07	$(0,0,1)(1,1,1)^{12}$	3,218.41	3,230.29
$(0,0,2)(1,1,1)^{12}$	3,181.48	3,196.32	$(0,0,1)(2,1,0)^{12}$	3,238.96	3,250.83
$(0,0,2)(2,1,1)^{12}$	3,180.41	3,198.22	$(0,0,1)(2,1,1)^{12}$	3,219.66	3,234.51
$(0,0,2)(0,1,1)^{12}$	3,179.52	3,191.39	$(0,0,1)(0,1,1)^{12}$	3,218.99	3,227.9
$(1,0,0)(1,1,1)^{12}$	3,172.85	3,184.72	$(1,0,0)(1,1,1)^{12}$	3,215.62	3,227.4
$(1,0,1)(0,1,1)^{12}$	3,164.26	3,176.13	$(1,0,0)(2,1,1)^{12}$	3,216.95	3,231.79
$(1,0,1)(1,1,1)^{12}$	3,165.74	3,180.58	$(1,0,0)(2,1,0)^{12}$	3,236.88	3,248.76
$(1,0,1)(2,1,1)^{12}$	3,163.58	3,181.4	$(1,0,1)(2,1,1)^{12}$	3,214.08	3,231.89
$(1,0,2)(1,1,1)^{12}$	3,165.4	3,183.22	$(1,0,1)(1,1,1)^{12}$	3,212.64	3,227.48
$(2,0,0)(1,1,1)^{12}$	3,172.47	3,187.31	$(1,0,1)(2,1,0)^{12}$	3,235.08	3,249.92
$(2,0,0)(2,1,1)^{12}$	3,170.87	3,188.68	$(1,0,2)(1,1,1)^{12}$	3,214.63	3,232.44
$(2,0,1)(0,1,1)^{12}$	3,164.56	3,179.41	$(2,0,0)(1,1,1)^{12}$	3,229.38	3,214.53
$(2,0,1)(1,1,1)^{12}$	3,166.05	3,183.87	$(2,0,0)(2,1,1)^{12}$	3,233.79	3,215.98
$(2,0,1)(2,1,1)^{12}$	3,164.04	3,184.83	$(2,0,0)(2,1,2)^{12}$	3,216.86	3,237.644
$(2,0,2)(0,1,1)^{12}$	3,165.43	3,183.24	$(2,0,1)(1,1,1)^{12}$	3,214.63	3,232.45
$(2,0,2)(1,1,1)^{12}$	3,167.08	3,187.87	$(2,0,1)(2,1,1)^{12}$	3,216.28	3,237.06
$(2,0,2)(2,1,1)^{12}$	3,165.23	3,188.98	$(2,0,1)(2,1,2)^{12}$	3,218.31	3,242.06
Best model			**Best model**		
$(1,0,1)(2,1,1)^{12}$	3,163.58	3,181.4	$(1,0,0)(1,1,1)^{12}$	3,215.62	3,227.4
			$(2,0,0)(1,1,1)^{12}$	3,229.38	3,214.53

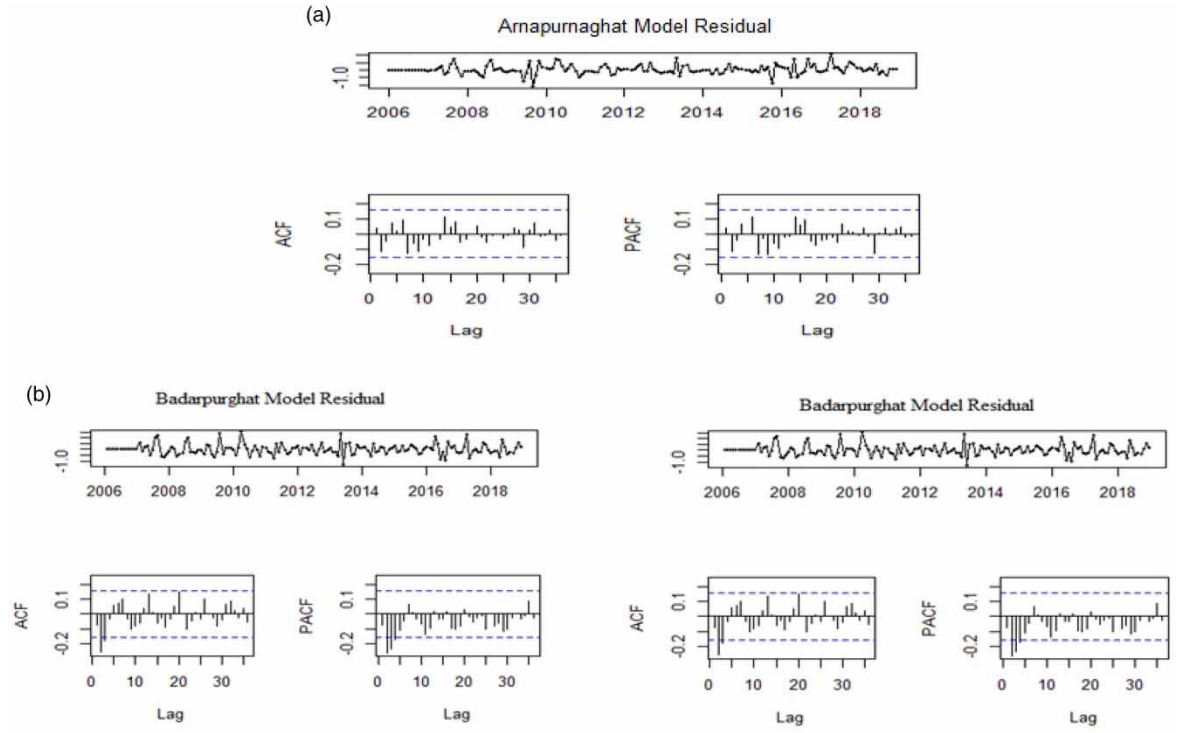

Figure 7 | (a) Annapurna residual test for best-fitted model. (b) Badarpurghat residual test for best-fitted model.

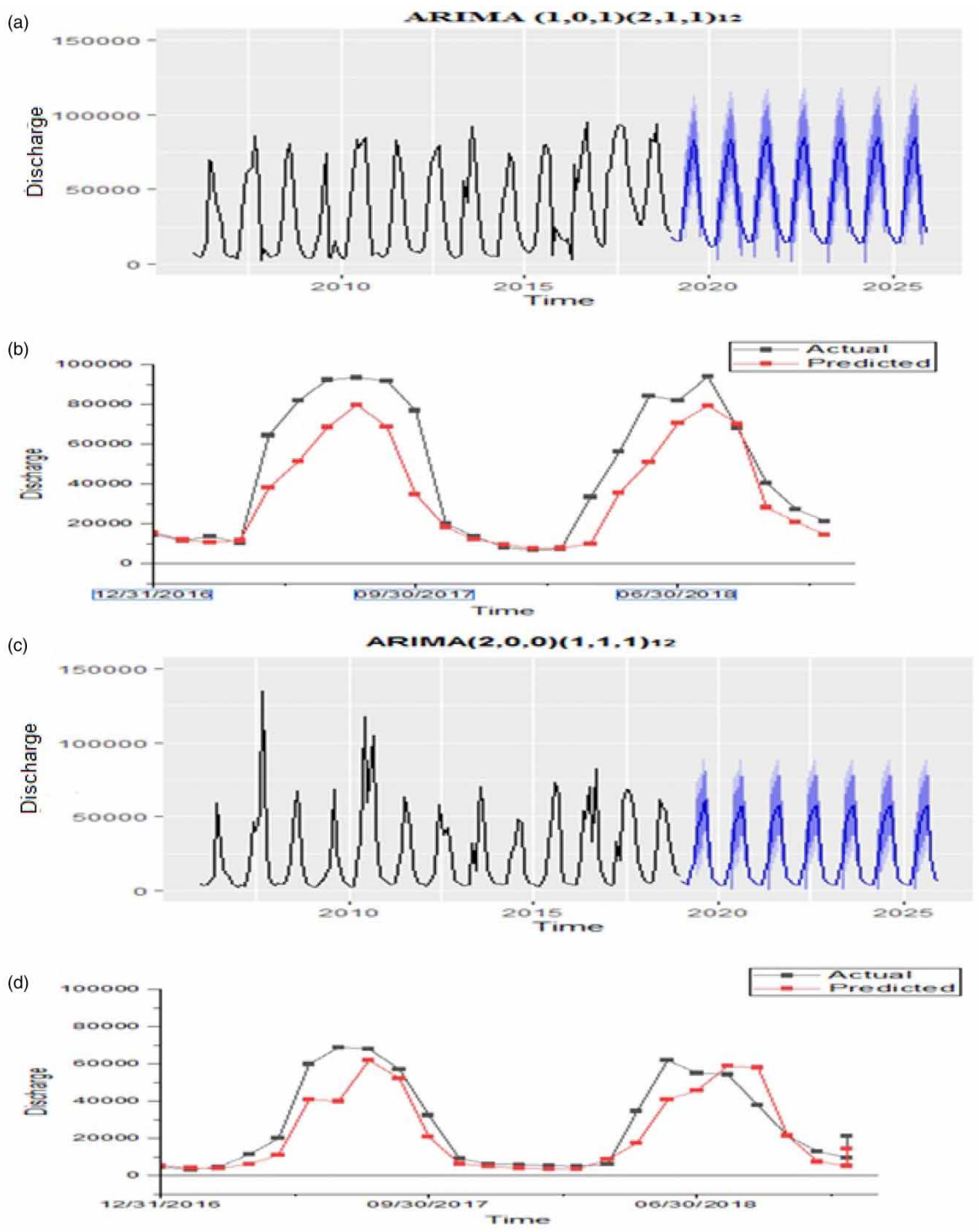

Figure 8 | (a) Forecasting discharge for Annapurna station. (b) Validation Annapurna discharge model. (c) Forecasting discharge for Badarpurghat station. (d) Validation Badarpurghat discharge model.

Table 5 | Performance of the chosen model

Model	R^2	MAPE
Arnapurnaghat station	0.83	29.78%
Badarpurghat station	0.87	23.52%

3.2.2. Forecast morphology

Now, the output of the discharge forecasted model was being used to analyze segment-by-segment future morphological assessment over the Barak River. According to the forecasting discharge for both stations, the upcoming discharge was expected to be quite high compared to the previous data trend. Because discharge is linked to erosion, it will directly impact river morphology.

Annapurnaghat river station was considered the upstream side of the study area, whereas the Badarpurghat river station was on the downstream side. The average high peak of the series was reported at Annapurnaghat station in August, at 2,197.46 m^3/s (CMS). The forecasted model's average peak, on the other hand, is 2,388.29 CMS. The lowest average discharge was recorded 235.89 CMS in February, but it increase upto 393.68 CMS for the forecasted model.

According to a previous segment-by-segment morphological study, DD and EE follow an incremental pattern. And both segments are primarily Silchar townships. Although a protective structure shields a section of the inside segments, more planning is necessary. According to morphological analysis, the segment CC was substantially less stable than the other sections. As a result, it is hazardous for those segments, as the forecasted model suggests an incremental discharge tendency. However, some portions of the bank are covered under a protection structure. But still, it will impact river morphology and increase the river's vulnerability rate soon.

The morphological study indicates that segment EE and FF have increased erosion during the last decade, particularly segment FF. As a result, effective erosion control preparation is required. In section GG, historical migration has already impacted the land. As a result, if the discharge is raised further, the segment will become more vulnerable. The developed discharge forecasted model also showed an incremental discharge pattern in the future.

4. CONCLUSION

The present study focused on segment-by-segment morphological assessment along the River Barak using remote sensing and GIS, as well as multi-temporal satellite data (Landsat). The effectiveness of recently protected zones within the study area, as well as future morphological assessments of the river Barak, was also investigated. The future morphological assessment was performed with the help of a developed river discharge forecasting model using SARIMA.

Morphological results show that where sinuosity indices decrease, bank erosion increases and vice versa. Thus, it influences the river's reach migration. The result shows that segment EE and segment FF, particularly segment FF, have eroded significantly in the recent decade. As a result, comprehensive erosion control preparation is required to protect future morphological changes. From the study, it was observed that the segment CC and segment GG were most vulnerable throughout the study period. Erosion protection structures at Sonabarighat Pt II, Sripur II, and Pachgram decrease erosional impacts even at high flow levels after installation. One of the most important concerns for the river management community is effective planning for vulnerable sections. As a result, it can be stated that implementing a protection system without sufficient planning will result in downstream vulnerability, as seen in the cases of Sonabarighat Pt I and Nizfulbari in this study. Forecasted discharge for the SARIMA model shows the upcoming incremental trend. It will also affect river morphology simultaneously. The stream gauge station Badarpurghat has lower uncertainty than Arnapurnaghat, according to the results of the uncertainty study. This study could be used as a primary informer for better river management in other alluvial rivers with similar characteristics. Results of the model may be improved using more datasets regarding river discharge, but limited data are available for this region.

ACKNOWLEDGEMENTS

We thank the Civil Engineering department of NIT Silchar for assistance throughout the research and the Department of Water Resources Department, Government of Assam for providing relevant data.

CONFLICT OF INTEREST

The author has no conflict of interest.

DATA AVAILABILITY STATEMENT

All relevant data are included in the paper or its Supplementary Information.

REFERENCES

Annayat, W. & Sil, B. S. 2020a Assessing channel morphology and prediction of centerline channel migration of the Barak River using geospatial techniques. *Bulletin of Engineering Geology and the Environment* **79**, 5161–5183. https://doi.org/10.1007/s10064-020-01894-9.

Annayat, W. & Sil, B. S. 2020b Changes in morphometric meander parameters and prediction of meander channel migration for the alluvial part of the Barak River. *Journal Geological Society of India* **96**, 279–291.

Bardhan, M. 1993 Channel stability of Barak river and its tributaries between Manipur-Assam and Assam-Bangladesh borders as seen from satellite imagery. In: *Proc. Nat. Syrup. on Remote Sensing Applications for Resource Management with Special Emphasis on N.E. Region, Held in Guwahati*, November 25–27, pp. 481–485.

Betancourt-Suárez, V., García-Botella, E. & Ramon-Morte, A. 2021 Flood mapping proposal in small watersheds: a case study of the RebollosandMiranda ephemeral streams (Cartagena, Spain). *Water* **13**, 102. https://doi.org/10.3390/w13010102.

Bhakal, L., Dubey, B. & Sarma, A. K. 2005 Estimation of bank erosion in the river Brahmaputra near Agyathuri by using geographic information system. *Journal of the Indian Society of Remote Sensing* **33** (1), 81–84.

Box, G. E. P. & Jenkins, G. M. 1976 *Time Series Analysis: Forecasting and Control*. Holden-Day, San Francisco.

Chatfield, C. 2000 *Time-Series Forecasting*, 1st edn. Chapman and Hall/CRC, Boca Raton, FL, USA. ISBN 978-1-4200-3620-6.

Choudhury, P., Roy, P. J., Nongthombam, J., Ullah, N., Devi, A. & Debbarman, S. 2014 *Flood Damage Mitigation: Report*. Assam State Disaster Management Authority.

Das, P. 2012 Study of Barak river meander and associated hazard around Silchar Town, Assam, using remote sensing and GIS. *Earth Science India* **5** (II), 51–59. EISSN: 0974–8350.

Das, P. K. 2013 North–East, The Power House of India': prospects and problems. *IOSR Journal of Humanities and Social Science (IOSR-JHSS)* **18** (3), 36–48. e-ISSN: 2279-0837, p-ISSN: 2279-0845.

Das, J. D. & Saraf, A. K. 2007 Remote sensing in the mapping of the Brahmaputra/Jamuna River channel patterns and its relation to various landforms and tectonic environment. *International Journal of Remote Sensing* **28**, 3619–3631.

Das, K. T., Halder, H. K. & Gupta, I. D. 2014 River bank erosion induced human displacement and its consequences. *Living Reviews in Landscape Research*. https://doi.org/10.12942lrlr-2014-3.

Dragicevic, S., Zivkovic, N., Roksandic, M., Kostadinov, S., Novkovic, I., Tosic, R., Stepic, M., Dragicevic, M. & Blagojevic, B. 2012 Land use changes and environmental problems caused by bank erosion: a case study of the Kolubara River Basin in Serbia. *Environmental Land Use Planning*. http://dx.doi.org/10.5772/50580.

Galavi, H., Mirzaei, M., Shui, L. T. & Valizadeh, N. 2013 Klang river–level forecasting using ARIMA and ANFIS models. *Journal – American Water Works Association*. doi:10.5942/jawwa.2013.105.0106.

Islam, F. & Rashid, A. N. M. 2011 Riverbank erosion displaces in Bangladesh: need for institutional response and policy intervention. *Bangladesh Journal of Bioethics* **2** (2), 4–19.

Kipgen, N. & Pegu, D. 2018 *Floods, Ecology and Cultural Adaptation in Lakhimpur District, Assam*. https://doi.org/10.1007/978-981-10-8485-0_20.

Klassen, G. J. & Verneer, K. 1988 Confluence scour in large braided rivers with fine bed materials. In *Presented at International Conference on Fluvial Hydraulics*. Budapest, pp. 395–408.

Kumar, D. & Bhattacharjya, R. K. 2020 Estimation of integrated flood vulnerability index for the hilly region of Uttarakhand, India. *Journal of Hazardous, Toxic, and Radioactive Waste* **24** (4), 04020051. doi:10.1061/(asce)hz.2153-5515.0000540.

Kummu, M., Lub, X. X., Rasphonec, A., Sarkkulad, J. & Koponen, J. 2008 Riverbank changes along the Mekong river: remote sensing detection in the Vientiane-NongKhai area. *Quaternary International* **186** (1), 100–112. doi:10.1016/j.quaint.2007.10.015.

Lane, S. N., Richards, K. S. & Chandler, J. H. 1995 Discharge and sediment supply controls on erosion and deposition in a dynamic alluvial channel. *Geomorphology* **15** (1), 1–15.

Laskar, A. A. & Phukon, P. 2012 Erosional vulnerability and spatio-temporal variability of the Barak River, NE India. *Current Science Association* **103** (1), 80–86.

Martínez-Acosta, L., Medrano-Barboza, J. P., López-Ramos, A., López, J. F. R. & López-Lambraño, A. A. 2020 SARIMA approach to generating synthetic monthly rainfall in the Sinú River watershed in Colombia. *Atmosphere* **11**, 602. doi:10.3390/atmos11060602.

Moeeni, H. & Bonakdari, H. 2010 Forecasting monthly inflow with extreme seasonal variation using the hybrid SARIMA-ANN model. *Stochastic Environmental Research and Risk Assessment* **2017** (31), 1997. doi:10.1007/s00477-016-1273-z.

Mohammed-Ali, W., Mendoza, C. & Holmes, R. R. 2020 Riverbank stability assessment during hydro-peak flow events: the lower Osage River case (Missouri, USA). *International Journal of River Basin Management*. Available from: https://www.tandfonline.com/toc/trbm20/19/3.

Mosavi, A., Ozturk, P. & Chau, K. 2018 Flood prediction using machine learning models: literature review. *Water* **10**, 1536. doi:10.3390/w10111536.

NDMA 2014 *Information on Floods*. Available from: http://www.ndma.gov.in/en/media-public-awareness/disaster/naturaldisaster.

Ozturk, D. & Sesli, F. A. 2015 Determination of temporal changes in the sinuosity and braiding characteristics of the Kizilirmak River, Turkey. *Polish Journal of Environmental Studies* **24** (5), 2095–2112.

Panda, P. C. & Bora, H. N. 1992 A study of sinuosity index of Siang River and its major tributaries: Arunachal Pradesh. *Environmental Management* **1**, 97–101.

Pati, J. K., Lal, J., Prakash, K. & Bhusan, R. 2008 Spatio-temporal shift of western bank of the Ganga river at Allahabad city and its implications. *Journal of the Indian Society of Remote Sensing* **36** (3), 289–297.

Prabhata, K. S., Ojha, C. S. P. & Ali, A. 1995 Mean annual flood estimation. *Journal of Water Resources Planning and Management* **121**, 403–407.

Rinaldi, M. 2003 Recent channel adjustments in Alluvial Rivers of Tuscany, Central Italy. *Earth Surface Processes and Landforms* **28** (6), 587–608. doi:10.1002/esp.464.

SAC and Brahmaputra Board 1996 *Report on Bank Erosion on Majuli Island, Assam: A Study Based on Multi Temporal Satellite Data*. Space Application Centre, Ahmedabad and Brahmaputra Board, Guwahati.

Sahoo, S. N. & Pekkat, S. 2018 Detention ponds for managing flood risk due to increased imperviousness: case study in an urbanizing catchment of India. *Nat. Hazards Rev*. **19** (1), 05017008. DOI: 10.1061/(ASCE)NH.1527-6996.0000271.

Schumm, S. A. 1963 *A Tentative Classification of Alluvial River Channels*. Geological survey circular 477.

Sharma, N., Johnson, F. A., Hutton, C. W. & Clark, M. 2010 Hazard vulnerability and risk on the Brahmaputra basin: a case study of river bank erosion. *The Open Hydrology Journal* **4**, 211–226.

Sharma, M. K., Mohammed, O. & Kiani, S. 2020 Time series analysis on precipitation with missing data using stochastic SARIMA. *MAUSAM* **71** (4), 617–624.

Stojković, M., Prohaska, S. & Plavšić, J. 2015 Stochastic structure of annual discharges of large European rivers. *Journal of Hydrology and Hydromechanics* **63** (1), 63–70.

Surian, N., Mao, L., Giacomin, M. & Ziliani, L. 2009 Morphological effects of different channel forming discharges in a gravel-bed river. *Earth Surface Processes and Landforms* **34**, 1093–1107. doi:10.1002/esp.1798.

Thalla, D., Thalla, A. K. & Devatha, C. P. 2010 Regional flood analysis: a case study of Narmada River Basin. In *EWRI 3rd International Perspective Current and Future State of Water Resource and Environment*.

WMO 2011 *World Meteorological Organization: Natural Hazards – Floods and Flash Floods*. Available from: http://www.wmo.int/pages/themes/hazards.

Yang, X., Damen, M. C. J. & van Zuidam, R. A. 1999 Satellite remote sensing and GIS for the analysis of channel. *International Journal of Applied Earth Observation and Geoinformation* **1** (2), 146–157. doi:10.1016/S0303-2434(99)85007-7

Yurekli, K., Kurunc, A. & Ozturk, F. 2005 Application of linear stochastic models to monthly flow data of Kelkit stream. *Ecological Modelling* **183** (1), 67–75.

Zhang, G. P. 2003 Time series forecasting using a hybrid ARIMA and neural network model. *Neurocomputing* **50**, 159–175.

First received 7 January 2022; accepted in revised form 30 April 2022. Available online 17 May 2022